Stem Cell Research (2008) 1, 116–128

available at www.sciencedirect.com

ScienceDirect

www.elsevier.com/locate/scr

p53 is required for etoposide-induced apoptosis of human embryonic stem cells

C. Grandela [a,b], M.F. Pera [b,c,d], E.J. Wolvetang [d,e,*]

[a] Doctoral Program in Experimental Biology and Biomedicine, Department of Zoology, Center for Neuroscience and Cell Biology, University of Coimbra, Coimbra, Portugal
[b] Monash Institute of Medical Research, School of Biomedical Sciences, Monash University, Clayton, Australia
[c] Center for Stem Cell and Regenerative Medicine, Keck School of Medicine, University of Southern California, Los Angeles, CA 90089, USA
[d] Australian Stem Cell Centre, Level 3 North Building 75 (STRIP), Wellington Road, Clayton, VIC 3168, Australia
[e] Department of Anatomy and Cell Biology, School of Biomedical Sciences, Monash University, Clayton, Australia

Received 30 July 2007; received in revised form 28 September 2007; accepted 8 October 2007

Abstract The molecular mechanisms controlling DNA-damage-induced apoptosis of human embryonic stem cells (hESC) are poorly understood. Here we investigate the role of p53 in etoposide-induced apoptosis. We show that p53 is constitutively expressed at high levels in the cytoplasm of hESC. Etoposide treatment results in a rapid and extensive induction of apoptosis and leads to a further increase in p53 and PUMA expression as well as Bax processing. p53 both translocates to the nucleus and associates with the mitochondria, accompanied by colocalization of Bax with Mcl1. hESC stably transduced with p53 shRNA display 80% reduction of endogenous p53 and exhibit an 80% reduction in etoposide-induced apoptosis accompanied by constitutive downregulation of Bax and an attenuated upregulation of PUMA. Our data further show that undifferentiated hESC that express Oct4 are much more sensitive to etoposide-induced apoptosis than their more differentiated progeny. Our study demonstrates that p53 is required for etoposide-induced apoptosis of hESC and reveals, at least in part, the molecular mechanism of DNA-damage-induced apoptosis in hESC.

Introduction

Human embryonic stem cell (hESC) lines are established from the inner cell mass of the blastocyst and differentiate into all cell lineages of the body. Although hESC grown under standard culture conditions on full-density feeder layers display unlimited self-renewal *in vitro*, they display remarkable genetic stability and do not show morphological changes characteristic of transformation. This could be due to both efficient DNA repair and the selective induction of apoptosis in hESC that have sustained DNA damage. DNA damage response and cell-cycle regulation differ markedly between mouse embryonic stem cells (mESC) and somatic cells (Hong and Stambrook, 2004). The spontaneous mutation frequency in mouse somatic cells is approximately 100-fold higher than in mESC. mESC also lack a G1 checkpoint and are hypersensitive to ionizing radiation and other DNA-damaging agents (Hong and Stambrook, 2004). These characteristics facilitate apoptosis and the removal of cells with a mutational burden from the population.

* Corresponding author. Australian Stem Cell Centre, Level 3 North Building 75 (STRIP), Wellington Road, Clayton, VIC 3168, Australia. Fax: +61 3 9271 1199.
E-mail address: ernst.wolvetang@stemcellcentre.edu.au (E.J. Wolvetang).

1873-5061/$ – see front matter
doi:10.1016/j.scr.2007.10.003

The tumor suppressor p53 plays a central role in suppressing tumorigenesis by inducing cell cycle arrest or apoptosis (Godefroy et al., 2004). Indeed, mutations of the p53 gene occur in approximately 50% of human cancers (Hollstein et al., 1991; Hussain and Harris, 1998; Levine, 1997). The role of p53 in guarding both mouse and human ES cells from the consequences of DNA-damage apoptosis remains largely unclear. While some investigators argue that p53 is nonfunctional in undifferentiated mESC (Aladjem et al., 1998), others show that p53 is involved in both UV-induced apoptosis (Chao et al., 2000; Xu et al., 2002) and differentiation (Sabapathy et al., 1997). Recently p53 was shown to be involved in UV-induced apoptosis of hESC (Qin et al., 2007) without modulation of p53 target gene expression.

The topoisomerase II inhibitor etoposide is an antineoplastic drug that has been widely used to couple DNA damage to apoptosis (Karpinich et al., 2002). Topoisomerase II is a nuclear enzyme that functions during both DNA replication and transcription (Hande, 1998). Topoisomerase II prevents "knots" from forming in DNA by allowing the passage of an intact segment of the helical DNA through a transient double-strand break (Burden and Osheroff, 1998). Etoposide stabilizes the complex formed by topoisomerase II and the 5′-cleaved ends of the DNA, thus forming stable (nonrepairable) protein-linked DNA double-strand breaks (Burden and Osheroff, 1998). Cells are able to recognize such DNA damage and, in turn, to eliminate the injured cells by p53-mediated apoptosis.

Induction of apoptosis by p53 can occur via both transcription-independent and transcription dependent pathways. The classical transcription-dependent pathway involves stabilization of p53 protein via a range of posttranslational modifications, nuclear translocation, and subsequent transactivation of proapoptotic genes, such as PUMA, Noxa, Bax, p53, AIP1, Apaf-1, and PERP, as well as repression of antiapoptotic genes such as Bcl2 and IAPs (Levine, 1997; Lu, 2005). p53 can also trigger apoptosis via a transcription-independent pathway that involves rapid translocation of a proportion of total cellular p53 directly to the mitochondria and interaction with the Bcl2 family of regulators of mitochondrial permeability (Chipuk et al., 2004; Erster et al., 2004; Leu et al., 2004; Mihara et al., 2003). Here we show that p53 is required for etoposide-induced apoptosis of hESC and that the p53 response in these cells involves both mitochondrial and nuclear apoptotic pathways.

Results

hESC are very sensitive to etoposide and exhibit classic apoptotic features

In response to inhibition of topoisomerase II with etoposide, hESC show an increase in apoptosis in a concentration- and time-dependent manner (Figs. 1A and 1B). Indeed, hESC appear to be far more sensitive to etoposide-induced apoptosis than other cell lines or primary cell cultures (Karpinich et al., 2002, 2006; Liu and Joel, 2003). As shown in Fig. S2C the human cell lines HT1080, 293FT, and CFPac-1 treated with 0.17 μM etoposide for 24 h display 3, 12, and 10% TUNEL-positive apoptotic cells, while hESC (HES-2) display more than 70% apoptosis after identical treatment, as also shown in Fig. 1B. Etoposide-induced apoptosis of hESC proceeds rapidly, with more than 70% of hESC undergoing apoptosis after 24 h incubation in the presence of 170 nM etoposide.

To confirm that hESC display hallmarks of apoptosis in response to DNA damage (see for review Lawen, 2003), we incubated hESC cultures with etoposide for various lengths of time and assessed mitochondrial cytochrome *c* release into the cytosol, caspase-3 activation, DNA laddering, and nuclear condensation. Incubation with etoposide (340 nM) for 3 h causes an increase in soluble cytochrome *c* in the cytosol of hESC, without affecting the total amount of intracellular cytochrome *c* (Fig. 1C). Furthermore, using an antibody specific to activated caspase-3 we show that hESC treated with etoposide for 3 h display caspase-3 activation and that this activation is inhibited by the general caspase inhibitor zVAD-fmk (Fig. 1D). By 3 to 4 h after addition of etoposide, hESC start to display the classical 210-bp DNA laddering pattern of apoptosis accompanied by the nuclear condensation (Fig. 1E) and fragmentation typical of apoptosis (Fig. 1F). There is no increase in necrotic cells over the time period during which we observed the four diagnostic features of apoptosis (Fig. 1G).

Etoposide-induced apoptosis of hESC requires caspase activation and is partially sensitive to cycloheximide

Cultures of hESC display a high rate of "spontaneous" apoptosis, with 15% of hESC undergoing apoptosis daily under optimal culture conditions. Caspases are centrally involved in the regulation and execution of the apoptotic program (Thornberry and Lazebnik, 1998) and caspase-3 is activated in etoposide-treated hESC cultures (Fig. 1D). To determine whether caspases play a functional role in etoposide-induced and spontaneous apoptosis of hESC, we incubated hESC with the general caspase inhibitor zVAD-fmk prior to etoposide treatment. As shown in Fig. 1H, zVAD-fmk totally inhibits etoposide-induced, but not spontaneous, apoptosis of hESC. Similarly, cycloheximide, an inhibitor of protein translation, is able to prevent 50% of etoposide-induced apoptosis but has no effect on spontaneous apoptosis. These data therefore indicate that hESC treated with etoposide undergo caspase- and protein translation-dependent apoptosis, whereas spontaneous apoptosis proceeds via caspase- and translation-independent pathways.

We did not observe any effect of bongkrekic acid (data not shown), an inhibitor of the adenine nucleotide translocator and mitochondrial permeability transition pore formation (Pastorino and Hoek, 2000; Scarlett et al., 2000), on spontaneous or etoposide-induced apoptosis of hESC. In agreement with this observation, we could not detect any loss of mitochondrial membrane potential, measured by JC-1 uptake, during the first 4 h of induction of apoptosis with etoposide (data not shown), despite the fact that cytochrome *c* release in the cytosol was already detected at 3 h. Cyclosporin A, an inhibitor of both mitochondrial permeability transition and calcineurin, induced apoptosis by itself and did not inhibit etoposide-induced apoptosis (results not shown). Preincubation with leptomycin B, a nuclear export inhibitor, or cyclic pifithrin-α, a purported inhibitor of p53-mediated transcription (Komarov et al., 1999), also had no or only a very minor inhibitory effect on etoposide-induced

hESC apoptosis. This is perhaps not surprising since the efficacy of pifithrin-α as an inhibitor of p53 transactivation activity is highly questionable (Walton et al., 2005). Pifithrin-μ, a compound that inhibits association of p53 with mitochondria (Strom et al., 2006), was found to reduce etoposide induced apoptosis of hESC by 50% (Fig. 1H).

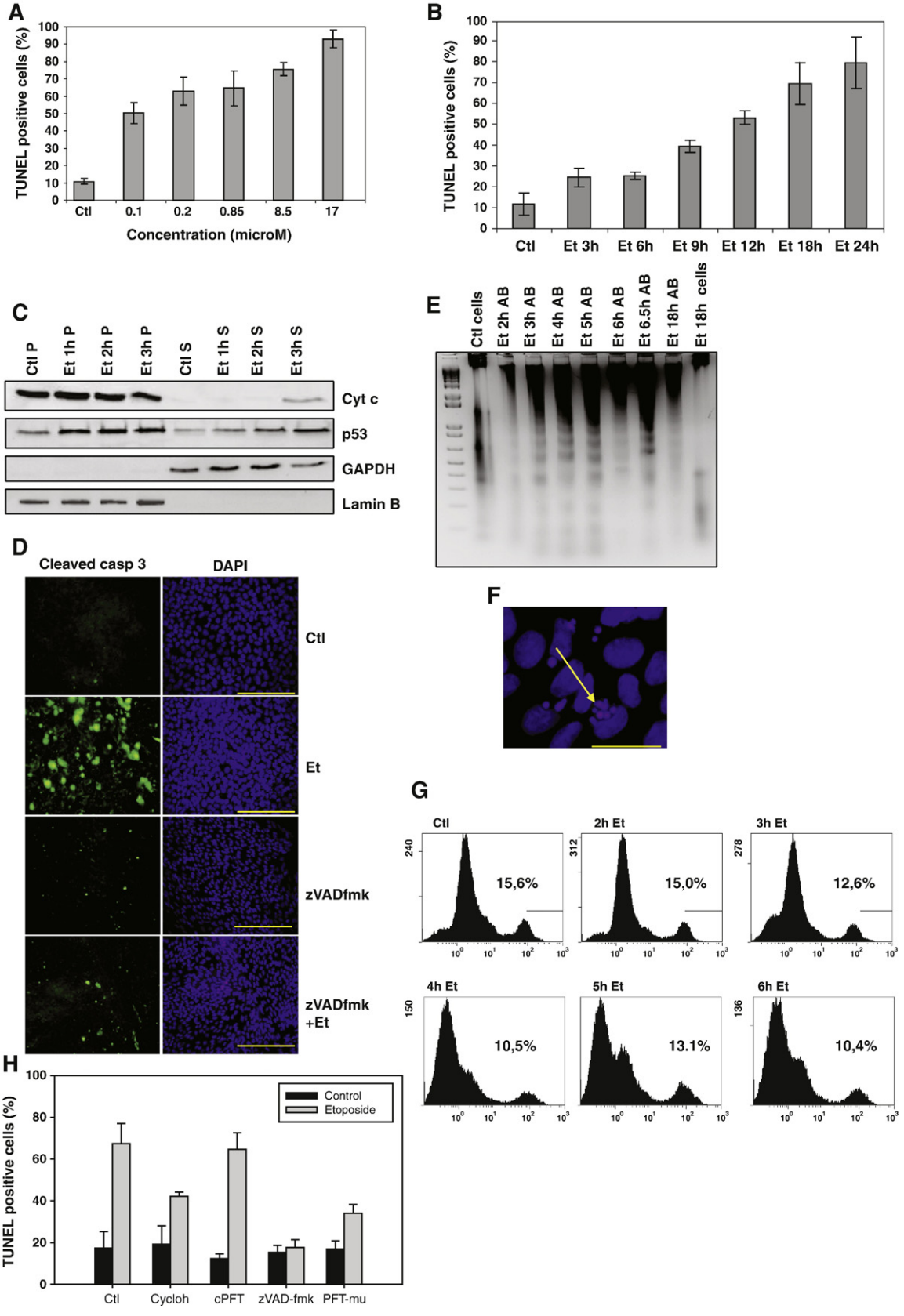

The state of differentiation of hESC affects their sensitivity to etoposide-induced apoptosis

hESC cultured on mouse embryonic fibroblast feeder cells in the presence of knockout serum replacement + 4 ng/ml b-FGF (Amit et al., 2004) appear to be a morphologically homogeneous population of undifferentiated cells. However, hESC cultured under these conditions are heterogeneous and display various degrees of differentiation as judged by the expression of the stem cell marker Oct4 when assayed by immunofluorescence and flow cytometry (Figs. S1 and S2). Cells at the outer rim of the hESC colonies display reduced expression of Oct4 and are more resistant to etoposide-induced apoptosis than undifferentiated hESC in the center of the colonies (Fig. S1A).

To quantify this phenomenon, we double-labeled etoposide-treated HES-2 and HES-4 cells with both TUNEL and antibody directed against the stem cell marker Oct4. As shown in Fig. 2, the survival of the Oct4-expressing hESC (~70% of the culture) was reduced to less than 10% within 18 h after etoposide treatment, which was accompanied by an increase in apoptosis from 10 to 70%. Within this time frame the proportion of surviving Oct4-negative cells was not significantly reduced, indicating that differentiated hESC are much more resistant to etoposide-induced apoptosis than their less differentiated counterparts. To highlight this effect of differentiation status on apoptosis we show the results for the HES-4 cell line, which displays a higher degree of spontaneous differentiation than other hESC lines. Similar results were obtained for the HES-2 cell line (data not shown).

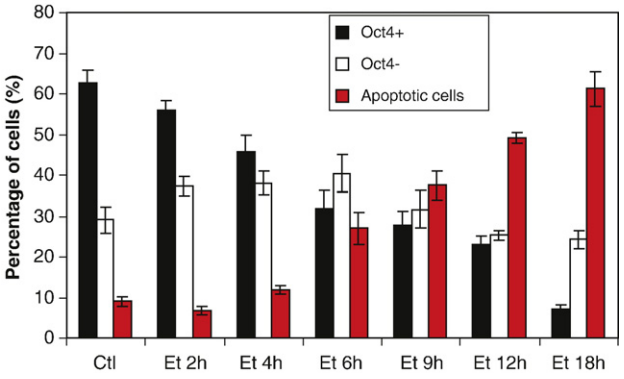

Figure 2 Differentiation of hESC reduces their sensitivity to etoposide-induced apoptosis. HES-4 cells were treated with 170 nM etoposide and harvested after 2, 4, 6, 9, 12, or 18 h. The etoposide-treated hESC were double-labeled with TUNEL and the stem cell marker Oct4 and analyzed by flow cytometry (see Supplemental Fig. S2A). The data are expressed as the percentage of surviving (TUNEL-negative) cells in the Oct4-positive and Oct4-negative fraction of the hESC culture. The results represent the means ± SD ($n = 3$). Similar results were obtained for HES-2 cells.

Expression analysis of several pro- and antiapoptotic proteins in hESC

To determine whether hESC express established regulators of p53-dependent apoptosis, we used immunostaining of *in situ*-fixed hESC cultures to detect proteins that are known to possess apoptotic or antiapoptotic activities. Fig. 3 shows that p53, Hdm2, Hdm4, Mcl1, Bax, and p14ARF are expressed in the HES-4 cell line, whereas Bcl2 was undetectable. Similar results were obtained for the HES-2 and HES-3 cell lines. In the majority of undifferentiated hESC, p53 has a cytoplasmic localization with only very few cells at the edge of the colonies displaying nuclear p53 staining detected by the DO-1 antibody. Similar results were obtained using a different anti-p53 antibody (pAB1801; Figs. 3B and 3C). The high levels of cytoplasmic expression of p53 in untreated hESC were confirmed by Western blotting of cytosolic protein extracts from hESC (Fig. 1C).

Figure 1 hESC are very sensitive to etoposide and exhibit classic apoptotic features. (A) Increasing etoposide concentrations between 0.1 and 17 μM for 18 h or (B) 170 nM etoposide for various time points between 3 and 24 h. Floating and adherent HES-3 (A) and HES-2 (B) cells were harvested after treatment, TUNEL stained, and analyzed by flow cytometry. Results shown are expressed as percentage means ± SD ($n = 3$). (C) Cytochrome *c* release. HES-2 cells were treated with 340 nM etoposide for 1, 2, or 3 h and permeabilized with digitonin. Proteins in the soluble (S—supernatant) and insoluble (P—pellet) fractions were resolved on separate 15% polyacrylamide gels and Western blotting was performed with p53, cytochrome *c*, lamin B (nuclear membrane protein), and GAPDH (cytosolic protein) antibodies. (D) Caspase-3 activation. HES-2 cells were preincubated with 25 μM zVAD-fmk or vehicle for 30 min and then treated with 340 nM etoposide for 3 h. PFA-fixed adherent colonies were immunostained for cleaved caspase-3 and nuclei visualized with DAPI. Scale bars, 200 μm. (E) DNA laddering. HES-2 cells were treated with 340 nM etoposide for 2 to 18 h and apoptotic bodies and cells were harvested at the indicated time points. DNA was collected and separated on a 1.5% agarose gel. A 1 kb DNA ladder (Invitrogen) was used as a size standard. (F) Chromatin condensation. HES-2 cells were treated with 340 nM etoposide for 6 h, fixed with 4% PFA, and stained with DAPI. The arrow indicates a human embryonic stem cell with the typical condensed fragmented appearance of an apoptotic cell. Scale bar, 50 μm. (G) Etoposide does not induce necrosis. HES-2 cells were treated with 340 nM etoposide for up to 6 h and apoptotic bodies and cells harvested at the indicated time points. Cells were then incubated with green fluorescence reactive dye (LIVE/DEAD Fixable Dead Cell stain) diluted in KSR medium for 30 min on ice in the dark, fixed in 3.7% PFA, and analyzed by flow cytometry. A representative experiment of three independent experiments is shown. (H) HES-2 cells were preincubated with vehicle alone or with inhibitor (25 μM zVAD-fmk for 30 min, 1 μg/ml cycloheximide for 30 min, 10 μM cyclic pifithrin-α (cPFT) for 1 h, or 10 μM pifithrin-μ for 1 h) and subsequently exposed to 170 nM etoposide for 18 h. Floating and adherent cells were harvested, stained with TUNEL, and analyzed by flow cytometry. Results are expressed as percentage means ± SD ($n = 3$). Similar results were obtained with HES-4 cells in each assay.

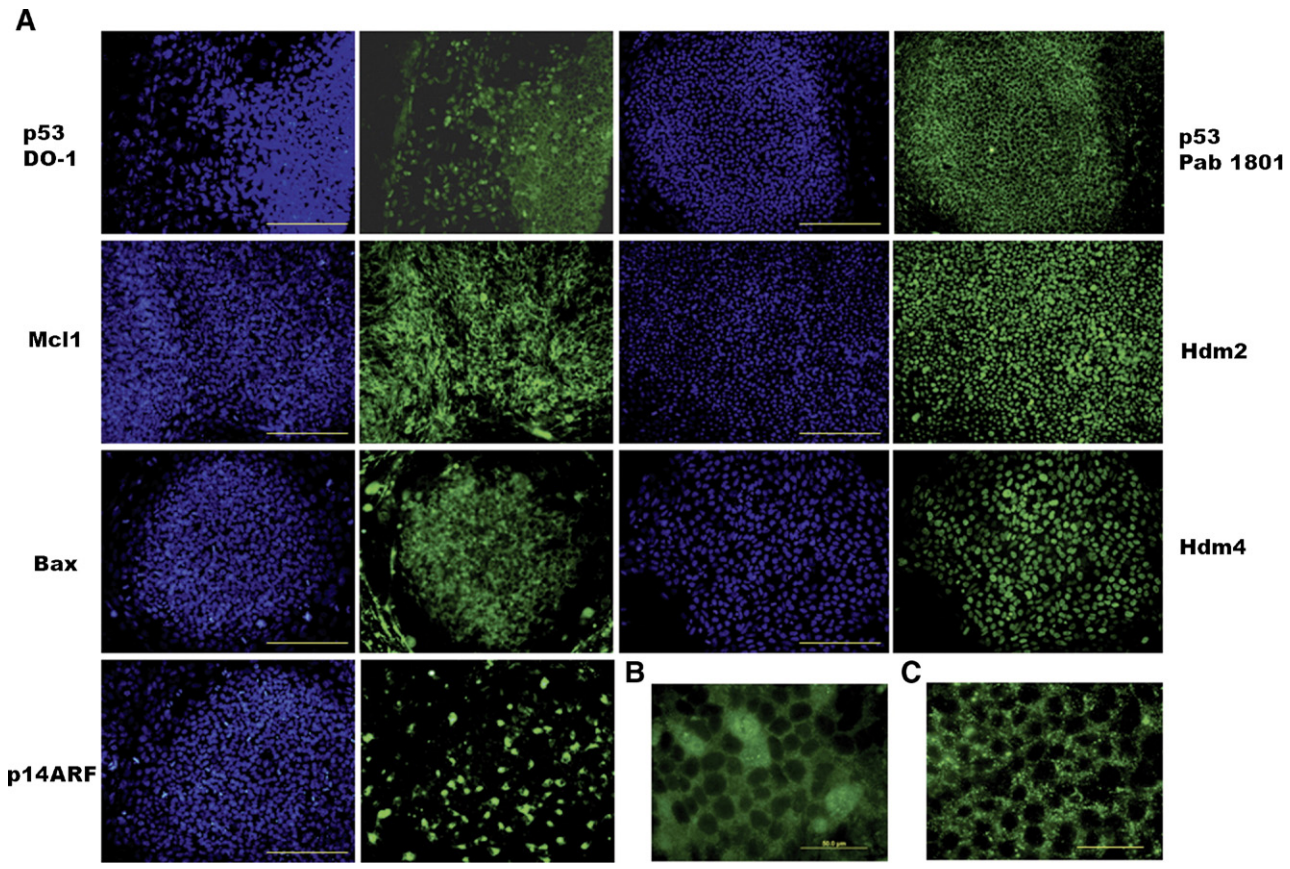

Figure 3 hESC exhibit a cytosolic localization of p53 and express Mcl1, Bax, p14ARF, Hdm4, and Hdm2 under standard culture conditions. (A) HES-4 colonies were fixed and immunostained for p53, Mcl1, Bax, p14ARF, Hdm4, and Hdm2. (B) and (C) represent higher magnifications of colonies immunostained with the antibodies p53 DO-1 and p53 pAB1801, respectively. Representative examples of three independent experiments are shown. Similar results were obtained with HES-2 and HES-3 cells. Scale bars, 200 μm.

Etoposide-induced apoptosis in hESC dramatically alters subcellular localization of p53, Bax, and Mcl1

In untreated undifferentiated hESC, p53 resides mainly in the cytosol in two forms, a soluble fraction and a particulate fraction, as judged by immunofluorescence detection (Fig. 3A) and cell fractionation (Fig. 1C). Four hours after etoposide treatment we detect colocalization of p53 with the mitochondrial marker antibody 1E6 (Banbury, 1994), suggesting that p53 associates with this organelle. During incubation with etoposide, the subcellular localization of the mitochondria themselves changes from a small punctate distribution throughout the cytosol to large aggregates of mitochondria in a perinuclear region that stain strongly for p53. Simultaneously, an increasing proportion of hESC display nuclear staining for p53 (Figs. 4A and 4B). These observations suggest that p53 translocates both to the mitochondria and to the nucleus in response to etoposide treatment. One of the prerequisites of mitochondrial permeability transition and cytochrome *c* release is thought to be the insertion of Bax into the outer mitochondrial membrane. When we examined the subcellular localization of Bax and Mcl1 between 3 and 18 h after etoposide treatment, Bax increasingly colocalized with Mcl1 in perinuclear structures reminiscent of the mitochondrial aggregates described above (Fig. 4C).

Altered expression of key apoptosis regulators upon etoposide-induced apoptosis in hESC

In most model systems, etoposide-induced apoptosis is dependent on p53 (Karpinich et al., 2002; Lowe et al., 1993; Yin et al., 2000). In agreement with these previous observations,

Figure 4 hESC show redistribution of cytosolic p53 to mitochondria and nucleus and colocalization of Mcl1 and Bax upon induction of apoptosis with etoposide. (A) HES-2 cells were exposed to 340 nM etoposide for 3 or 18 h, PFA-fixed, and immunostained for p53 and nuclei (DAPI). Representative examples of three independent experiments are shown. Similar results were obtained with HES-4 cells. Scale bars, 100 μm. (B) Confocal microscope images of HES-2 cells treated with 340 nM etoposide for 4 h. p53 relocalizes from the cytosol to the nucleus as well as to the mitochondria (1E6 is a mitochondrial marker). Scale bars, 50 μm. (C) HES-4 cells were exposed to 340 nM etoposide for 3 and 18 h, PFA-fixed, and immunostained for Mcl1, Bax, and nuclei (DAPI). Upon induction of apoptosis with etoposide, Mcl1 and Bax colocalize in a perinuclear region in structures reminiscent of mitochondrial aggregates. Scale bars, 100 μm (control and 3 h 340 nM etoposide) and 50 μm (18 h 340 nM etoposide).

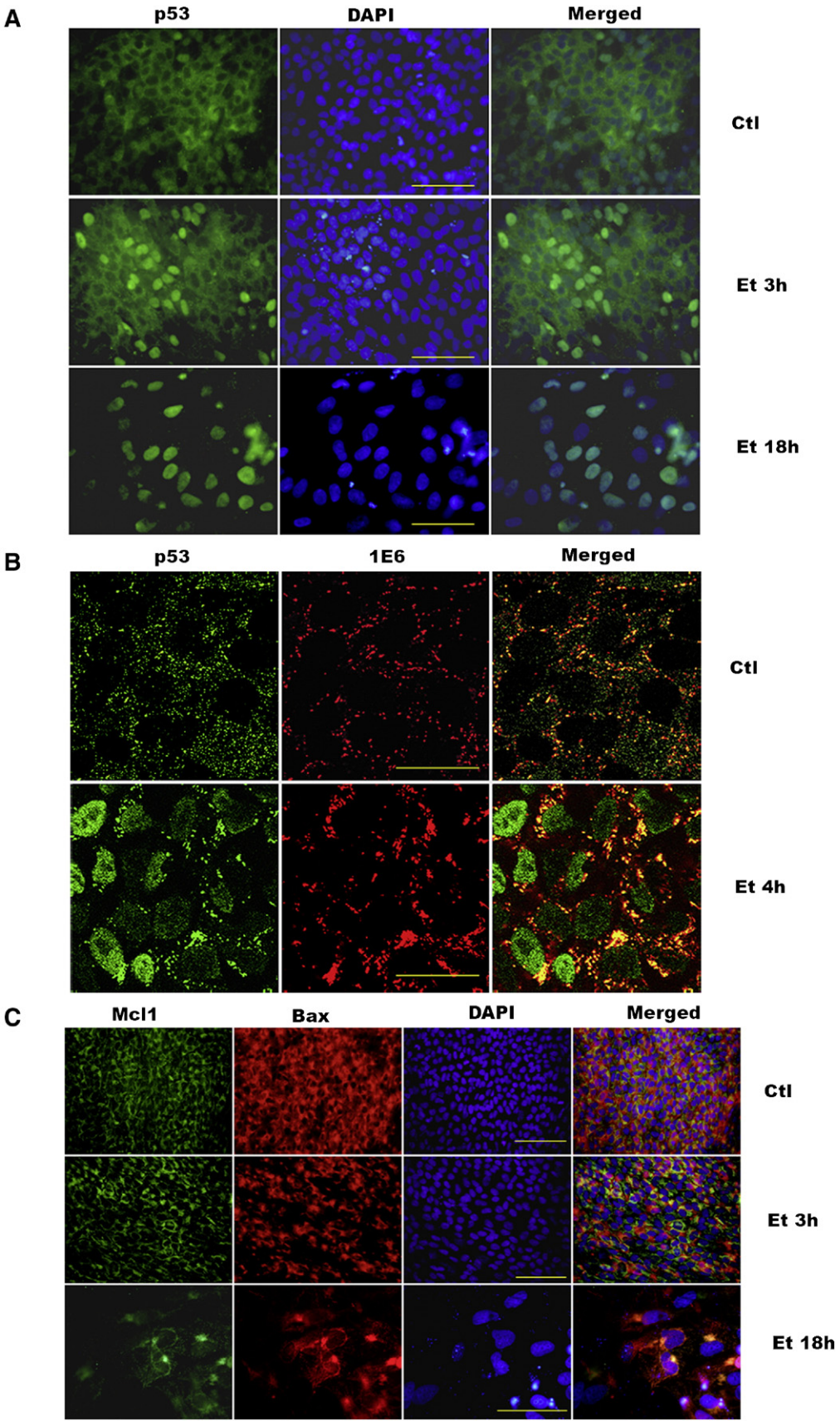
A
p53
DAPI
Merged
Ctl
Et 3h
Et 18h
B
p53
1E6
Merged
Ctl
Et 4h
C
Mcl1
Bax
DAPI
Merged
Ctl
Et 3h
Et 18h

we detect an increase in p53 expression as early as 3 h after etoposide addition. Expression of p53 then peaks around 6–9 h of exposure to etoposide and wanes thereafter (Fig. 5A). PUMA, one of the downstream targets of p53, is upregulated between 4.5 and 6 h after exposure to etoposide, as is nuclear p53. Furthermore, consistent with the release of cytochrome *c* at 3 h after exposure to etoposide, increased activation of caspase-3 is maintained for 6 to 8 h after etoposide addition. Similar kinetics of upregulation was observed for Hdm2. By contrast, no alteration in Mcl1, Hdm4, Noxa, or Oct4 expression was found in etoposide-treated hESC (Fig. 5A). However, Nanog was downregulated in hESC after etoposide-induced upregulation of p53, in agreement with the previously reported (Lin et al., 2005) ability of p53 to suppress Nanog expression in mESC. We detect no, or only very slight, upregulation of the p53 target Bax in response to etoposide treatment but a clear increase in processing of Bax to the more potent proapoptotic 18-kDa form with time (Gao and Dou, 2000; Wood and Newcomb, 2000). We did not detect expression of p21, a potential downstream target of p53 involved in cell cycle arrest in many cellular model systems, in either untreated or etoposide-treated hESC by Western blotting or immunofluorescence (data not shown). This was not due to an inability of the antibody to detect p21, since we could detect robust expression of p21 in protein extracts of human embryonic fibroblasts (data not shown). Since cycloheximide is able to inhibit 50% of etoposide-induced apoptosis, we were interested in determining how this relates to the expression of p53-regulated apoptosis modulators. As shown in Fig. 5B preincubation with cycloheximide does not prevent the upregulation of p53, suggesting that the majority of its increased expression is due to increased stabilization of p53 protein and not to *de novo* synthesis. However, the expression of Bax, PUMA, and Mcl1 is clearly reduced by this protein synthesis inhibitor, suggesting that Bax and PUMA may be important determinants of etoposide-induced apoptosis of hESC.

p53 is required for etoposide-induced apoptosis

To investigate the role of p53 in etoposide-induced apoptosis of hESC we stably transduced HES-2 hESC with a lentivirus carrying short hairpin RNA (shRNA) designed to knock down p53 mRNA. As shown in Figs. 6B and 6C, p53 shRNA-transduced hESC (i) constitutively express only 20% of p53 protein compared to untransduced or control GFP shRNA-transduced hESC and (ii) display a reduced upregulation of p53 in response to etoposide addition. These data are consistent with the 80% reduction in etoposide-induced apoptosis observed in p53 shRNA-transduced hESC (Fig. 6A). These data demonstrate that etoposide-induced apoptosis of hESC is dependent on p53. The reduction of p53-dependent apoptosis in the p53 shRNA-transduced hESC is accompanied by a constitutive downregulation of Bax expression and an attenuated upregulation of PUMA in response to etoposide addition. These data therefore strongly suggest that the reduction of etoposide-induced apoptosis in p53-knockdown hESC is due to a reduced upregulation of PUMA and a constitutively reduced expression of Bax. The reduced sensitivity of the p53 shRNA-transduced hESC to etoposide-induced apoptosis is not due to an increased differentiation.

p53 is required for spontaneous apoptosis

Between 10 and 15% of hESC (HES-2, HES-3, and HES-4) grown under standard serum-free culture conditions (Amit et al., 2004) undergo spontaneous apoptosis over an 18-h period. As shown in Fig. 6, HES-2 stably transduced with p53 shRNA and displaying only 20% residual p53 expression compared to untransduced or GFP shRNA-transduced hESC display a reduction in spontaneous apoptosis from 11.4±5.4 to only 2.4±1.0% (Fig. 6A). GFP shRNA-transduced HES-2 cells or nontransduced hESC continued to display 15% spontaneous apoptosis, indicating that the reduction in spontaneous apoptosis is not due to the lentiviral transduction per se. Although the reason for the relatively high rate of spontaneous apoptosis in hESC serum-free culture is unknown, our data indicate that spontaneous apoptosis is dependent on p53.

Transcriptome analysis of GFP and p53 shRNA-transduced hESC

Three replicates of hESC (HES-2 and HES-4) transduced with either GFP or p53 shRNA were FACS sorted using the cell surface markers CD9 and GCTM2 to obtain a population of undifferentiated hESC. RNA was isolated from these fractions and subjected to microarray analysis on the 46K Human Illumina platform. The data shown in Fig. S3 demonstrate that biological replicates of transduced lines display highly similar transcriptome profiles and that a similar set of genes was consistently altered between p53 and GFP shRNA-transduced lines, independent of the HES lines used. Indeed, 70% of differentially expressed genes were found to contain p53 binding sites in their promoters. A selection of five consistently differentially expressed genes between GFP and p53 shRNA-transduced hESC is shown in the table in Fig. S3. These p53-regulated genes were previously shown to exhibit binding of p53 to consensus p53 binding sites in their promoters by CHIP analysis (Wei et al., 2006).

Discussion

hESC are highly susceptible to spontaneous and etoposide-induced apoptosis

p53 is considered a critical regulator of genomic integrity because of its ability to trigger apoptosis and/or cell cycle arrest in response to genotoxic stress. Because embryonic stem cells display remarkable genomic stability and are highly sensitive to ionizing radiation and other DNA-damaging agents we examined in detail the role of p53 in the regulation of apoptosis of human embryonic stem cells. To this end we opted to use etoposide treatment since this drug has been shown to activate the p53 pathway specifically in many model systems. Our data demonstrate that etoposide apoptosis of hESC requires p53. We further show that hESC display the characteristic features of apoptosis and, like mESC, are extremely sensitive to both spontaneous and etoposide-induced apoptosis. Spontaneous apoptosis of cultured hESC is mediated by p53, since reduction of p53 expression in HES-2 causes a commensurate reduction in apoptosis. These data are in agreement with a recent study by Qin et al.

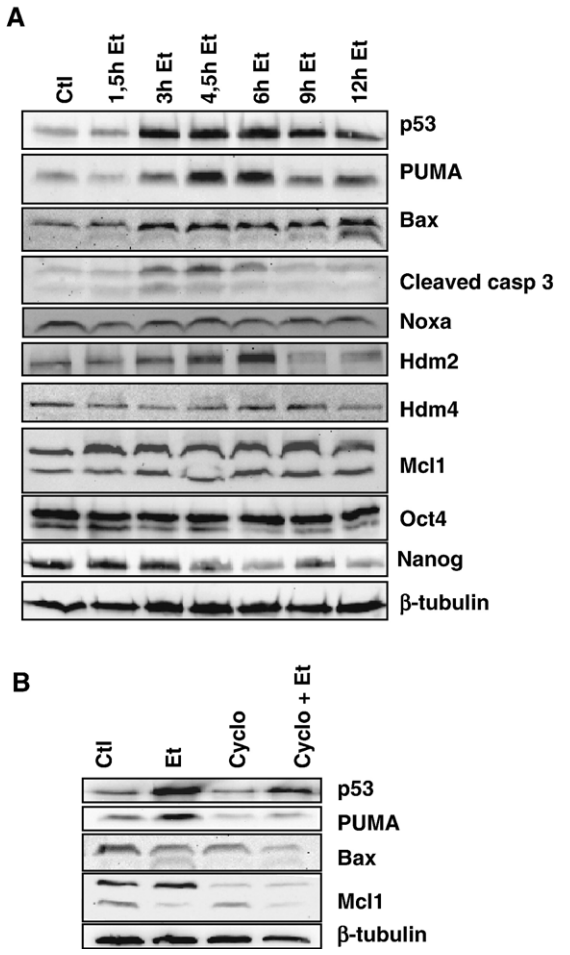

Figure 5 Increased expression of p53, processing of Bax, and altered expression of p53 downstream targets PUMA, Hdm2, and Nanog in hESC treated with etoposide. (A) HES-2 cells were harvested 1.5, 3, 4.5, 6, 9, and 12 h after treatment with 170 nM etoposide. Protein extracts were resolved on separate polyacrylamide gels and Western blotted with antibodies against p53, PUMA, Bax, cleaved caspase-3, Hdm2, Hdm4, Mcl1, and Oct4. β-Tubulin was used to ensure equal loading. A representative example of three independent experiments is shown. (B) Cycloheximide treatment interferes with etoposide-induced upregulation of PUMA and Bax in hESC. HES-2 cells were preincubated with (Cyclo) or without 1 μg/ml cycloheximide (Ctl) for 30 min and treated with 170 nM etoposide (Et) for 18 h. Protein extracts were resolved on separate polyacrylamide gels and Western blotted with antibodies against p53, Mcl1, Bax, PUMA, and β-tubulin. A representative example of three independent experiments is shown.

(2007), who also showed that spontaneous and UV-induced apoptosis of hESC is controlled by p53. If p53-mediated spontaneous apoptosis is involved in eliminating genetically damaged cells from the stem cell population, reduction of p53 function should result in an increased frequency of chromosomal abnormalities and genetic mutations. We are currently testing this hypothesis. The karyotypes of the GFP shRNA-transduced control HES-2 and p53 shRNA-transduced HES-2 cells were found to be normal at weekly passage 13 (results not shown).

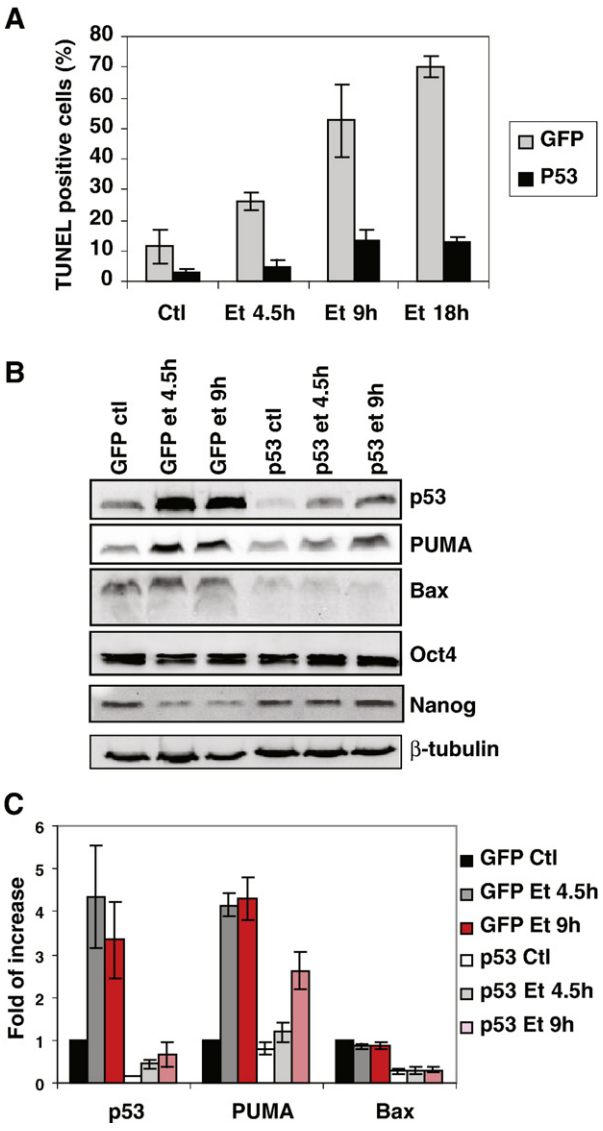

Figure 6 p53 is required for etoposide-induced apoptosis of hESC. (A) HES-2 cells were stably transduced with lentivirus carrying shRNA designed to knock down p53 or GFP. Both p53 shRNA-transduced and GFP shRNA-transduced (control) hESC were harvested 4.5, 9, and 18 h after treatment with 170 nM etoposide. Cells were subsequently PFA-fixed, labeled with TUNEL, immunostained with the stem cell marker Oct4, and analyzed by flow cytometry. Results shown are expressed as percentage means ± SD ($n = 4$). (B) Downregulation of p53 and p53 downstream targets Bax and PUMA in p53 shRNA-transduced HES-2 cells. HES-2 cells stably expressing p53 shRNA or GFP shRNA were harvested 4.5 and 9 h after treatment with 170 nM etoposide. Protein extracts were boiled in Laemmli buffer, resolved on separate polyacrylamide gels, and analyzed by Western blotting with p53, PUMA, Bax, Nanog, and Oct4 antibodies. β-Tubulin was used to ensure equal protein loading. (C) Quantification of protein expression using software-based densitometric analysis on cross-reactive bands and the β-tubulin loading controls. A representative example of three independent experiments is shown.

Differentiation of hESC reduces their sensitivity to etoposide-induced apoptosis

The sensitivity of hESC (HES-2 and HES-4) to etoposide-induced apoptosis is dependent on their differentiation status. We show that undifferentiated hESC that express Oct4 are the least resistant to etoposide-induced apoptosis compared to their more differentiated progeny. Clearly the reduction in Oct4 immunoreactivity in apoptotic hESC observed in flow-cytometric analysis 6–9 h after etoposide treatment is not due to an increase in differentiation, which proceeds much more slowly over a period of days. Indeed, when analyzed by Western blotting, Oct4 protein expression was not reduced (Fig. S2B). Given the profound effect of the differentiation status of hESC on their rate of apoptosis we strongly argue that meaningful data on apoptosis in hESC can be obtained only when TUNEL-labeled cells are double labeled with at least one pluripotency marker, as performed in this study. In agreement with our data, undifferentiated mESC were recently shown to be more sensitive to *O*(6)-methylguanine-induced apoptosis than their differentiated counterparts (Roos et al., 2007).

Our data further show that p53 has a small but reproducible effect on spontaneous differentiation of cultured hESC as determined by the slight increase in Oct4 expression by FACS in p53 shRNA-transduced hESC lines (91.7±3.4% (n=5)) compared to the GFP shRNA-transduced controls (83.4±3.2% (n=5), $p<0.01$), similar to what was observed by Qin et al. (2007).

The mechanism of p53-dependent apoptosis in hESC

Initiation of etoposide-induced apoptosis in hESC commences around 3 h after etoposide addition with translocation of the highly expressed cytosolic p53 protein to the mitochondria and release of cytochrome *c*. There is no detectable loss of mitochondrial membrane potential, as judged by the maintenance of JC-1 red/green fluorescence. Cytochrome *c* release from mitochondria without loss of mitochondrial membrane potential has previously been reported (Finucane et al., 1999; Grubb et al., 2001; Krohn et al., 1999). Because caspase-3 is activated at 3 h after etoposide treatment, we conclude that apoptosome formation and initiation of the apoptotic cascade has already commenced at this stage. The dramatic increase in nuclear p53, which occurs at the same time, suggests that there are two fractions of cytosolic p53 with different functions in apoptosis induction in response to etoposide: one that associates with the mitochondria and one that translocates to the nucleus. In support of this idea, inhibition of p53 association with mitochondria with pifithrin-μ prevents only 50% of etoposide-induced apoptosis of hESC (Fig. 1H). Nuclear accumulation of p53 is accompanied by an early upregulation of the p53 target gene PUMA, but does not cause an increase in p21. This finding may explain why cells that have initiated apoptosis fail to arrest the cell cycle in G0/G1 (as indicated by flow-cytometric analysis of DAPI-stained hESC cultures (data not shown)). In this respect hESC resemble mouse ES cells (Xu et al., 2002), which also do not exhibit cell cycle arrest or slowdown upon UV-induced DNA damage. The fact that we observe modulation of only a subset of p53 target genes (PUMA, Hdm2, Nanog) in response to p53 upregulation suggests that p53 exhibits target specificity, which may be due, for example, to differences in p53 posttranslational modifications, histone modifications, or interactions with other transcription factors.

Our data are in contrast to the study by Qin et al. (2007), which indicated that UV- and γ-radiation-induced apoptosis of hESC, although p53 dependent, does not lead to accumulation of Bax or Hdm2 and does not cause activation of any p53 downstream target genes in luciferase reporter assays. The authors postulated that posttranslational modifications of p53 render the p53 protein transcriptionally inactive without interfering with p53's ability to repress Oct4 and Nanog expression. It was consequently concluded that p53 induces apoptosis solely through a mitochondrial pathway. We find, however, that, similar to what we observe for etoposide-induced apoptosis, γ-radiation (1 Gy)-induced apoptosis of hESC causes increased p53 expression that is accompanied by upregulation of the p53 downstream target genes PUMA and Hdm2 (Fig. S3B). These differences may be due to intrinsic cell line differences (H1 hESC vs HES-2, HES-3, and HES-4 in our study), the passage number of the hESC (p42–68 H1 vs less than p15 in our study), or the method of propagation (dispase vs collagenase in our study). Indeed, there is an increasing amount of evidence to suggest that hESC can adapt to culture conditions with increasing time in culture (Baker et al., 2007) and that these changes can impact on the regulation of apoptosis (Herszfeld et al., 2006). Alternatively, some of the differing data between the two studies may be due to mechanistic differences between the responses of hESC to the different apoptotic stimuli, namely UV irradiation and etoposide treatment (Attardi et al., 2004). For example, UVB treatment generally causes activation of p38 and/or wip1 (Takekawa et al., 2000). p38-mediated phosphorylation and stabilization of p53 can subsequently cause cytoplasmic sequestration of wild-type p53, leading to an absence of p53 target gene modulation (Chouinard et al., 2002), while wip1 expression has been shown to suppress both p53-mediated transcription and apoptosis in response to UV radiation (Takekawa et al., 2000). Neither p38 nor WIP1 has previously been implicated in etoposide-induced apoptosis.

Microarray analysis of untreated p53 shRNA-knockdown hESC and GFP shRNA-transduced control hESC shows that there are highly similar sets of up- and downregulated mRNAs in both HES-2 and HES-4 p53 shRNA-transduced hESC in three independent biological replicates (Fig. S3). Bioinformatic analysis shows that more than 70% of these genes contain p53 binding sites in their promoters. We have highlighted five p53-regulated genes that were previously shown to bind p53 in their promoters (Wei et al., 2006). These data strongly suggest that the observed gene expression changes are not due to viral insertion effects and that even without etoposide treatment p53 is involved in the regulation of several known p53-controlled genes.

hESC express high levels of p53 protein in the cytosol under standard culture conditions. In mESC, cytoplasmic p53 protein translocates inefficiently to the nucleus upon nucleotide depletion and the cells undergo p53-independent apoptosis in response to DNA damage. This response is clearly different in hESC, which show an increase in nuclear p53 expression after etoposide treatment. This may be due to differences between the DNA-damage response mechanisms in etoposide-treated

cells and in cells exposed to nucleotide depletion or to intrinsic differences between mouse and human ES cells. Reduction of the pool of p53 by lentivirally delivered shRNA leads to a reduced expression of Bax and an attenuated upregulation of PUMA after etoposide treatment, suggesting that these proteins may be critical p53 downstream targets for induction of etoposide-induced apoptosis in hESC. In other model systems PUMA, a BH3-only derepressor molecule, counteracts the antiapoptotic function of Mcl1 and induces a proapoptotic conformational change in Bax (Kuwana et al., 2005). BH3-only Bcl2 family members such as PUMA trigger mitochondrial cytochrome *c* release without loss of mitochondrial membrane potential (Shimizu and Tsujimoto, 2000), as is the case in etoposide-treated hESC. Alternatively PUMA may be involved in the release of mitochondrially associated p53 to enhance nuclear p53-mediated apoptotic events further, as recently demonstrated by Chipuk et al. (2005).

hESC represent a unique cellular model to study p53 regulation of apoptosis, given that they are nontransformed immortal cells with a normal karyotype and cannot be directly compared to long-established cell lines, in which apoptosis pathways are intrinsically altered as part of the transformation process, or even to primary cell cultures, which display senescence, DNA-damage-induced cell cycle arrest, and contact inhibition. The regulation and kinetics of apoptosis in hESC are very similar to those observed for *in vivo*-irradiated thymocytes, with a rapid p53 transcription-independent first wave of apoptosis followed by a second p53 transcription-dependent wave (Erster et al., 2004) and a very early upregulation of PUMA and Bax coincident with caspase-3 activation. Our data suggest that in hESC these two waves occur either simultaneously or very soon one after the other. In both model systems, however, the p53-dependent upregulation of PUMA and Bax appears to be a critical determinant. We propose a working model for etoposide-induced apoptosis in hESC (Fig. 7) in which DNA damage leads to stabilization and increased expression of p53 followed by translocation of p53 to both the mitochondria, where it possibly interacts with Mcl1, and the nucleus, where it leads to transcriptional upregulation of PUMA and maintenance of Bax expression. The 18-kDa processed forms of Bax and PUMA next cooperate in triggering cytochrome *c* release from the mitochondria without loss of membrane potential and this subsequently leads to activation of a caspase-3-dependent apoptotic program. The presence of two simultaneous pathways to induce p53-mediated apoptosis may be a failsafe mechanism of hESC to ensure that abnormal hESC do not contribute to the developing tissues and the germ line.

Material and methods

Cell culture

hES cell lines HES-2, HES-3, and HES-4 (Reubinoff et al., 2000) were cultured (a) on a mouse fibroblast feeder (MEF) layer at a density of 6×10^4 cells/cm^2 in DMEM with 20% FCS, 1% ITS, 1% pen/strep, 1% l-glutamine, 1% NEAA, and 0.1 mM β-mercaptoethanol using mechanical transfer or (b) with a mouse fibroblast feeder density of 2×10^4 cells/cm^2 in KSR medium with 20% KO-serum replacement, 1% l-glutamine, 1% NEAA, 4 ng/ml b-FGF, and 0.1 mM β-mercaptoethanol using 4 mg/ml collagenase (Worthington Biochemical) for serial passaging (Amit et al., 2000). Cells were plated on Matrigel (BD Biosciences) with MEF-conditioned serum replacement medium as described (Xu et al., 2001). hES cell lines were used only up to passage 15 when cultured as per Amit et al. (2000) or Xu et al. (2001).

DNA laddering

hESC and apoptotic bodies were collected and washed with PBS. DNA laddering was determined using standard protocol 2 as described at http://www.sgul.ac.uk/depts/immunology/~dash/group/laddering.html.

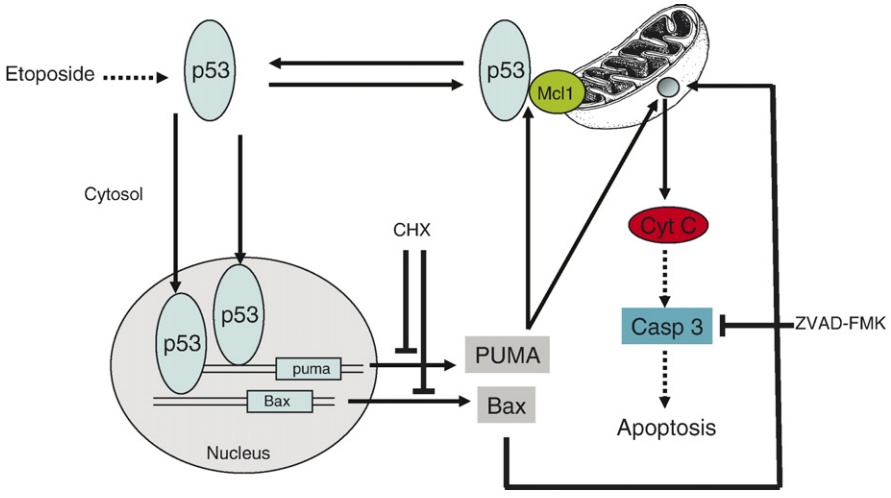

Figure 7 A model depicting the role of p53 and p53 downstream targets in the regulation of etoposide-induced apoptosis of hESC. In response to DNA damage p53 translocates to both the mitochondria, where it possibly interacts with Mcl1, and the nucleus, where it triggers upregulation of PUMA and maintenance of Bax expression. PUMA and Bax subsequently cooperate in facilitating cytochrome *c* release without loss of membrane potential and initiation of the apoptotic cascade. See text for details.

Cell subfractionation

hESC were washed with PBS and permeabilized with 20 μg/ml digitonin for 10 min at 37 °C. The cytosolic/soluble fraction was collected and boiled in Laemmli sample buffer. Cells were washed twice with PBS and boiled in Laemmli sample buffer (insoluble fraction).

Immunofluorescence

hESC were fixed with 4% paraformaldehyde (PFA) for 20 min, washed with PBS, incubated with the primary or isotype-control antibody at the indicated dilution for least 2 h at 21 °C, and visualized using appropriate secondary fluorescent antibodies. Primary antibodies were used at the following dilutions: p53, 1:50 (DO-1; Santa Cruz Biotechnology); p53, 1:100 (Pab 1801; Abcam); Mcl1, 1:50 (Abcam); Bax, 1:50 (DAKO); cleaved caspase-3 (Asp175), 1:100 (Cell Signaling); Bcl2, 1:50 (Santa Cruz Biotechnology); Mdm2, 1:50 (Abcam); p21, 1:50 (BD Pharmingen); Oct4, 1:40 (Santa Cruz Biotechnology); and mitochondrial marker antibody 1E6, undiluted (Banbury, 1994). Cells were subsequently counterstained with DAPI (1 μg/ml), mounted with Vectashield mounting medium (Vector), and analyzed using a fluorescence microscope (FluorMicro BX51; Olympus).

Western blotting analysis

hESC were harvested with Cell Dissociation Solution (Sigma) and boiled in Laemmli buffer. Proteins were separated by electrophoresis through 12% SDS–PAGE gels and electrotransferred to Hybond P (Amersham). The membranes were blocked with 4% skim milk powder and incubated with primary antibody overnight at 4 °C and reactivity was visualized using appropriate HRP-conjugated secondary antibodies and ECL (Amersham). The primary antibodies, respective dilutions, and sources were p53, 1:1000 (DO-1; Santa Cruz Biotechnology); Mcl1, 1:1000 (Abcam); Hdm2, 1:1000 (SMP14; Sigma); Hdm4, 1:1000 (Abcam); Bax, 1:1000 (DAKO); cleaved caspase-3 (Asp175), 1:1000 (Cell Signaling); β-tubulin, 1:50,000 (Sigma); lamin B, 1:1000 (Calbiochem); GAPDH, 1:4000 (Ambion); cytochrome *c*, 1:200 (BD Pharmingen); PUMA, 1:1000 (Calbiochem); Bcl2, 1:1000 (Santa Cruz Biotechnology); p21, 1:1000 (BD Pharmingen). Images were acquired using the Bio-Rad Gel ChemiDoc XRS System. Last, software-based densitometric analysis (Gel-Pro Analyser version 3.1; MediaCybernetics) was performed on cross-reactive bands and the β-tubulin loading controls.

Apoptosis and flow cytometry analysis

Etoposide (Sigma) was used as an apoptosis-inducing agent. After the various treatments, adherent cells and floating cells were harvested with Cell Dissociation Solution (Sigma), pooled, and pelleted by centrifugation. Suspensions were subsequently fixed with PFA (2%) and permeabilized with 0.1% Triton X-100 for TUNEL (Roche) labeling as described by the manufacturer and additional labeling with Oct4 1:40 (Santa Cruz Biotechnology) prior to analysis by flow cytometry (Cytometrics FC 500 System; Beckman Coulter). Cyclic pifithrin-α (c-PFT, 10 μM; Sigma), pifithrin-μ (10 μM; Calbiochem), and bongkrekic acid (50 μM; Sigma) were added 1 h before the treatment with etoposide. zVAD-fmk (25 μM; Sigma) and cycloheximide (1 μg/ml; Sigma) were added 30 min before the treatment with etoposide.

Measurement of mitochondrial membrane potential

The MitoProbe JC-1 (5,5′,6,6′-tetrachloro-1,1′,3,3′-tetraethylbenzimidazolylcarbocyanine iodide) assay kit for flow cytometry (Invitrogen) was used to measure mitochondrial membrane potential according to the manufacturer's instructions. Cells were analyzed by flow cytometry (Cytometrics FC 500 System; Beckman Coulter). In control experiments, cells were incubated with the ionophore carbonyl cyanide 3-chlorophenylhydrazone at 100 μM 5 min prior to the addition of JC-1.

Cell staining for viability

The LIVE/DEAD Fixable Dead Cell stain kit (green fluorescence; Invitrogen) was used to distinguish apoptosis from necrosis. The assay was performed according to the manufacturer's instructions. Cells were analyzed by flow cytometry (Cytometrics FC 500 System; Beckman Coulter).

Lentiviral shRNAi

HES-2 cells were transduced with lentivirus carrying shRNA designed to knock down p53 or GFP using the Block-It Lentiviral RNAi Expression System (Invitrogen), as described by the manufacturer. The p53 shRNA sequences used were the following: p53 top strand, 5′-CGCGCACAGAGGAAGAGAATCTCGAAAGATTCTCTTCCTCTGTGTGCGC-3′, and p53 bottom strand, 5′-AAAAGCGCACAGAGGAAGAGAATCTTTTCGAGATTCTCTCTTCCTCTGTGCGC-3′; GFP top strand, 5′-CACCGAAGAAGTCGTGCTGCTTCATCGAAATGAAGCAGCACGACTTCTTC-3′, and GFP bottom strand, 5′-AAAAGAAGAAGTCGTGCTGCTTCATTTCGATGAAGCAGCACGACTTCTTC-3′.

Cells were plated on Matrigel and infected with lentivirus (m.o.i. of 3). Selection with blasticidin (5 μg/ml) was performed for 1 week after each infection and cells were transferred to flasks with MEF feeders at 2×10^4 cells/cm^2 in KSR medium. Apoptosis assays and Western blotting analysis were performed as described above.

Acknowledgments

We thank Irene Tellis, Karen Koh, and Linh Nguyen (Monash University) and Pegah Jamshidi, Lisa Kass, and Tracy Lomas (ASCC) for expert technical assistance in hESC cell line culture; Andrew Fryga (ASCC) for discussion on flow cytometry; Ygal Haupt for helpful discussion and suggestions; Joe Sambrook for critically reading the manuscript; George Thouas for cyclosporin and CCCP; and João Ramalho-Santos for facilitating this research. We greatly acknowledge Sean Grimmond and Gabriel Kolle for their transcriptome and bioinformatic analyses. This work was supported partially by the Fundação para a Ciência e a Tecnologia, Portugal, and Catarina Grandela is a recipient of a Ph.D. fellowship from the

Fundação para a Ciência e Tecnologia (Portugal). The ASCC is greatly acknowledged for financial and material support.

Appendix A. Supplementary data

Supplementary data associated with this article can be found, in the online version, at doi:10.1016/j.scr.2007.10.003.

References

Aladjem, M.I., Spike, B.T., Rodewald, L.W., Hope, T.J., Klemm, M., Jaenisch, R., Wahl, G.M., 1998. ES cells do not activate p53-dependent stress responses and undergo p53-independent apoptosis in response to DNA damage. Curr. Biol. 8, 145–155.

Amit, M., Carpenter, M.K., Inokuma, M.S., Chiu, C.P., Harris, C.P., Waknitz, M.A., Itskovitz-Eldor, J., Thomson, J.A., 2000. Clonally derived human embryonic stem cell lines maintain pluripotency and proliferative potential for prolonged periods of culture. Dev. Biol. 227, 271–278.

Amit, M., Shariki, C., Margulets, V., Itskovitz-Eldor, J., 2004. Feeder layer- and serum-free culture of human embryonic stem cells. Biol. Reprod. 70, 837–845.

Attardi, L.D., de Vries, A., Jacks, T., 2004. Activation of the p53-dependent G1 checkpoint response in mouse embryo fibroblasts depends on the specific DNA damage inducer. Oncogene 23, 973–980.

Baker, D.E., Harrison, N.J., Maltby, E., Smith, K., Moore, H.D., Shaw, P.J., Heath, P.R., Holden, H., Andrews, P.W., 2007. Adaptation to culture of human embryonic stem cells and oncogenesis *in vivo*. Nat. Biotechnol. 25, 207–215.

Banbury, D.N., 1994. New Monoclonal Antibodies to Visualize Vesicular Compartments. Univ. of Oxford, Oxford. [PhD thesis].

Burden, D.A., Osheroff, N., 1998. Mechanism of action of eukaryotic topoisomerase II and drugs targeted to the enzyme. Biochim. Biophys. Acta 1400, 139–154.

Chao, C., Saito, S., Kang, J., Anderson, C.W., Appella, E., Xu, Y., 2000. p53 transcriptional activity is essential for p53-dependent apoptosis following DNA damage. EMBO J. 19, 4967–4975.

Chipuk, J.E., Bouchier-Hayes, L., Kuwana, T., Newmeyer, D.D., Green, D.R., 2005. PUMA couples the nuclear and cytoplasmic proapoptotic function of p53. Science 309, 1732–1735 (See comment).

Chipuk, J.E., Kuwana, T., Bouchier-Hayes, L., Droin, N.M., Newmeyer, D.D., Schuler, M., Green, D.R., 2004. Direct activation of Bax by p53 mediates mitochondrial membrane permeabilization and apoptosis. Science 303, 1010–1014.

Chouinard, N., Valerie, K., Rouabhia, M., Huot, J., 2002. UVB-mediated activation of p38 mitogen-activated protein kinase enhances resistance of normal human keratinocytes to apoptosis by stabilizing cytoplasmic p53. Biochem. J. 365, 133–145.

Erster, S., Mihara, M., Kim, R.H., Petrenko, O., Moll, U.M., 2004. In vivo mitochondrial p53 translocation triggers a rapid first wave of cell death in response to DNA damage that can precede p53 target gene activation. Mol. Cell. Biol. 24, 6728–6741.

Finucane, D.M., Waterhouse, N.J., Amarante-Mendes, G.P., Cotter, T.G., Green, D.R., 1999. Collapse of the inner mitochondrial transmembrane potential is not required for apoptosis of HL60 cells. Exp. Cell Res. 251, 166–174.

Gao, G., Dou, Q., 2000. N-terminal cleavage of bax by calpain generates a potent proapoptotic 18-kDa fragment that promotes bcl-2-independent cytochrome C release and apoptotic cell death. J. Cell. Biochem. 80, 53–72.

Godefroy, N., Lemaire, C., Renaud, F., Rincheval, V., Perez, S., Parvu-Ferecatu, I., Mignotte, B., Vayssiere, J.L., 2004. p53 can promote mitochondria- and caspase-independent apoptosis. Cell Death Differ. 11, 785–787.

Grubb, D.R., Ly, J.D., Vaillant, F., Johnson, K.L., Lawen, A., 2001. Mitochondrial cytochrome c release is caspase-dependent and does not involve mitochondrial permeability transition in didemnin B-induced apoptosis. Oncogene 20, 4085–4094.

Hande, K.R., 1998. Etoposide: four decades of development of a topoisomerase II inhibitor. Eur. J. Cancer 34, 1514–1521.

Herszfeld, D., Wolvetang, E., Langton-Bunker, E., Chung, T.L., Filipczyk, A.A., Houssami, S., Jamshidi, P., Koh, K., Laslett, A.L., Michalska, A., Nguyen, L., Reubinoff, B.E., Tellis, I., Auerbach, J.M., Ording, C.J., Looijenga, L.H., Pera, M.F., 2006. CD30 is a survival factor and a biomarker for transformed human pluripotent stem cells. Nat. Biotechnol. 24, 351–357.

Hollstein, M., Sidransky, D., Vogelstein, B., Harris, C.C., 1991. p53 mutations in human cancers. Science 253, 49–53.

Hong, Y., Stambrook, P.J., 2004. Restoration of an absent G1 arrest and protection from apoptosis in embryonic stem cells after ionizing radiation. Proc. Natl. Acad. Sci. U. S. A. 101, 14443–14448.

Hussain, S.P., Harris, C.C., 1998. Molecular epidemiology of human cancer: contribution of mutation spectra studies of tumor suppressor genes. Cancer Res. 58, 4023–4037.

Karpinich, N.O., Tafani, M., Rothman, R.J., Russo, M.A., Farber, J.L., 2002. The course of etoposide-induced apoptosis from damage to DNA and p53 activation to mitochondrial release of cytochrome c. J. Biol. Chem. 277, 16547–16552.

Karpinich, N.O., Tafani, M., Schneider, T., Russo, M.A., Farber, J.L., 2006. The course of etoposide-induced apoptosis in Jurkat cells lacking p53 and Bax. J. Cell. Physiol. 208, 55–63.

Komarov, P.G., Komarova, E.A., Kondratov, R.V., Christov-Tselkov, K., Coon, J.S., Chernov, M.V., Gudkov, A.V., 1999. A chemical inhibitor of p53 that protects mice from the side effects of cancer therapy. Science 285, 1733–1737.

Krohn, A.J., Wahlbrink, T., Prehn, J.H., 1999. Mitochondrial depolarization is not required for neuronal apoptosis. J. Neurosci. 1, 7394–7404.

Kuwana, T., Bouchier-Hayes, L., Chipuk, J.E., Bonzon, C., Sullivan, B.A., Green, D.R., Newmeyer, D.D., 2005. BH3 domains of BH3-only proteins differentially regulate Bax-mediated mitochondrial membrane permeabilization both directly and indirectly. Mol. Cell 17, 525–535.

Lawen, A., 2003. Apoptosis—an introduction. BioEssays 25, 888–896.

Leu, J.I., Dumont, P., Hafey, M., Murphy, M.E., George, D.L., 2004. Mitochondrial p53 activates Bak and causes disruption of a Bak–Mcl1 complex. Nat. Cell Biol. 6, 443–450.

Levine, A.J., 1997. p53, the cellular gatekeeper for growth and division. Cell 88, 323–331.

Lin, T., Chao, C., Saito, S., Mazur, S.J., Murphy, M.E., Appella, E., Xu, Y., 2005. p53 induces differentiation of mouse embryonic stem cells by suppressing Nanog expression. Nat. Cell Biol. 7, 165–171.

Liu, W.M., Joel, S.P., 2003. The schedule-dependent effects of etoposide in leukaemic cell lines: a function of concentration and duration. Cancer Chemother. Pharmacol. 51, 291–296.

Lowe, S.W., Ruley, H.E., Jacks, T., Housman, D.E., 1993. p53-dependent apoptosis modulates the cytotoxicity of anticancer agents. Cell 74, 957–967.

Lu, X., 2005. p53: a heavily dictated dictator of life and death. Curr. Opin. Genet. Dev. 15, 27–33.

Mihara, M., Erster, S., Zaika, A., Petrenko, O., Chittenden, T., Pancoska, P., Moll, U.M., 2003. p53 has a direct apoptogenic role at the mitochondria. Mol. Cell 11, 577–590.

Pastorino, J.G., Hoek, J.B., 2000. Ethanol potentiates tumor necrosis factor-alpha cytotoxicity in hepatoma cells and primary rat hepatocytes by promoting induction of the mitochondrial permeability transition. Hepatology 31, 1141–1152.

Qin, H., Yu, T., Qing, T., Liu, Y., Zhao, Y., Cai, J., Li, J., Song, Z., Qu, X., Zhou, P., Wu, J., Ding, M., Deng, H., 2007. Regulation of apoptosis and differentiation by p53 in human embryonic stem cells. J. Biol. Chem. 282, 5842–5852.

Reubinoff, B.E., Pera, M.F., Fong, C.Y., Trounson, A., Bongso, A., 2000. Embryonic stem cell lines from human blastocysts: somatic

differentiation in vitro [erratum appears in Nat. Biotechnol. 2000 18, 559]. Nat. Biotechnol. 18, 399–404 (See comment).

Roos, W.P., Christmann, M., Fraser, S.T., Kaina, B., 2007. Mouse embryonic stem cells are hypersensitive to apoptosis triggered by the DNA damage O(6)-methylguanine due to high E2F1 regulated mismatch repair. Cell Death Differ. 14, 1422–1432.

Sabapathy, K., Klemm, M., Jaenisch, R., Wagner, E.F., 1997. Regulation of ES cell differentiation by functional and conformational modulation of p53. EMBO J. 16, 6217–6229.

Scarlett, J.L., Sheard, P.W., Hughes, G., Ledgerwood, E.C., Ku, H.H., Murphy, M.P., 2000. Changes in mitochondrial membrane potential during staurosporine-induced apoptosis in Jurkat cells. FEBS Lett. 475, 267–272.

Shimizu, S., Tsujimoto, Y., 2000. Proapoptotic BH3-only Bcl-2 family members induce cytochrome c release, but not mitochondrial membrane potential loss, and do not directly modulate voltage-dependent anion channel activity. Proc. Natl. Acad. Sci. 97, 577–582.

Strom, E., Sathe, S., Komarov, P.G., Chernova, O.B., Pavlovska, I., Shyshynova, I., Bosykh, D.A., Burdelya, L.G., Macklis, R.M., Skaliter, R., Komarova, E.A., Gudkov, A.V., 2006. Small-molecule inhibitor of p53 binding to mitochondria protects mice from gamma radiation. Nat. Chem. Biol. 2, 474–479.

Takekawa, M., Adachi, M., Nakahata, A., Nakayama, I., Itoh, F., Tsukuda, H., Taya, Y., Imai, K., 2000. p53-inducible wip1 phosphatase mediates a negative feedback regulation of p38 MAPK–p53 signaling in response to UV radiation. EMBO J. 19, 6517–6526.

Thornberry, N.A., Lazebnik, Y., 1998. Caspases: enemies within. Science 281, 1312–1316.

Walton, M.I., Wilson, S.C., Hardcastle, I.R., Mirza, A.R., Workman, P., 2005. An evaluation of the ability of pifithrin-alpha and -beta to inhibit p53 function in two wild-type p53 human tumor cell lines. Mol. Cancer Ther. 4, 1369–1377.

Wei, C.L., Wu, Q., Vega, V.B., Chiu, K.P., Ng, P., Zhang, T., Shahab, A., Yong, H.C., Fu, Y., Weng, Z., Liu, J., Zhao, X.D., Chew, J.L., Lee, Y.L., Kuznetsov, V.A., Sung, W.K., Miller, L.D., Lim, B., Liu, E.T., Yu, Q., Ng, H.H., Ruan, Y., 2006. A global map of p53 transcription-factor binding sites in the human genome. Cell 124, 207–219.

Wood, D.E., Newcomb, E.W., 2000. Cleavage of Bax enhances its cell death function. Exp. Cell Res. 256, 375–382.

Xu, C., Inokuma, M.S., Denham, J., Golds, K., Kundu, P., Gold, J.D., Carpenter, M.K., 2001. Feeder-free growth of undifferentiated human embryonic stem cells. Nat. Biotechnol. 19, 971–974.

Xu, D., Wilson, T.J., Chan, D., De Luca, E., Zhou, J., Hertzog, P.J., Kola, I., 2002. Ets1 is required for p53 transcriptional activity in UV-induced apoptosis in embryonic stem cells. EMBO J. 21, 4081–4093.

Yin, D., Tamaki, N., Kokunai, T., 2000. Wild-type p53-dependent etoposide-induced apoptosis mediated by caspase-3 activation in human glioma cells. J. Neurosurg. 93, 289–297.